photonics

MDPI

Communication

Phototherapy of Brain Tumours Using a Fibre Optic Neurosystem

Yuliya Maklygina [1,*], Igor Romanishkin [1], Aleksej Skobeltsin [1], Dina Farrakhova [1] and Victor Loschenov [1,2]

[1] Prokhorov General Physics Institute of the Russian Academy of Sciences, 119991 Moscow, Russia; igor.romanishkin@ncs.gpi.ru (I.R.); skoaleksej@yandex.ru (A.S.); farrakhova.dina@mail.ru (D.F.); loschenov@mail.ru (V.L.)

[2] National Research Nuclear University MEPhI, Department №87, 115409 Moscow, Russia

* Correspondence: jmclygina@ncs.gpi.ru; Tel.: +7-977-803-76-27

Abstract: In this work, a new approach was tested to assess the cellular composition of tissues by time-resolved methods of fluorescence analysis of exogenous and endogenous fluorophores. First of all, the differences in fluorescence kinetics of endogenous fluorophores (coenzymes NADH and FAD) in tumour and immunocompetent cells were determined. After that, differences in fluorescence kinetics of photosensitizer 5 ALA-induced protoporphyrin IX were established due to its different metabolism in cells of different phenotypes. Kinetics of photoluminescence of NADH and FAD coenzymes as well as photosensitizer were studied by means of two different methods: time-resolved spectroscopy based on a streak-camera and fibre optic neuroscopy, which served to perform process monitoring and regular fluorescence diagnosis of the probed region. Time-resolved fluorescence microscopy (FLIM) was used as a control technique. Time-resolved spectroscopic fluorescence lifetime analysis was performed on sexually mature female rats induced with glioma C6 brain tumour under in vivo conditions; thus, under conditions where the immune system actively intervenes in the process of oncogenesis. In this regard, the aim of the study was to recognize the cellular composition of the brain tumour tissue, namely the ratio of cancer and immunocompetent cells and their mutual localization. Understanding the role of the immune system thus provides new ways and approaches for further diagnosis and therapy, making tumour-associated immune cells a prime target for modern therapies.

Keywords: fibre optic neurosystem; time-resolved laser spectroscopy; laser confocal microscopy; photosensitizers; endogenous fluorophores (NADH, FAD); spectral-resolved microimages of malignant neural tissue tumours; tumour-associated macrophages/microglia

Citation: Maklygina, Y.; Romanishkin, I.; Skobeltsin, A.; Farrakhova, D.; Loschenov, V. Phototherapy of Brain Tumours Using a Fibre Optic Neurosystem. *Photonics* **2021**, *8*, 462. https://doi.org/10.3390/photonics8110462

Received: 20 September 2021
Accepted: 18 October 2021
Published: 21 October 2021

1. Introduction

Optical spectroscopy techniques, especially time-resolved optical spectroscopy, for the analysis of brain condition and function have significant advantages over other techniques used in neurosurgery and neuro-oncology [1–4]. One important advantage is the high speed of information processing. Equally important is the wide range of physiological and morphological parameters available for optical spectroscopy analysis. These methods allow for a clear correlation between the recorded signal—absorption, fluorescence or different types of scattering due to both substances originally inherent to neural tissues and cells and contrasting markers introduced from outside—and small and rapid functional changes in the examined tissues, and show a strong correlation with the profound metabolic and structural rearrangements that take place in the development of brain pathologies [5–7]. In particular, time-resolved spectroscopy and microscopy make it possible to assess, by recording the fluorescence lifetime of externally injected photosensitizers, the condition of tissues that differ in phenotype due to their different metabolism and the nature of interaction with photosensitizer molecules [8–10].

However, the specificity of brain tumours lies in their difficult accessibility and depth of embedding. In this regard, a neurosystem with an intracranial fibre structure has been

previously developed that enables one to deliver laser radiation to a considerable depth inside the brain tissue after its intracranial implantation [11].

Thus, laser fluorescence methods and devices with picosecond temporal resolution seem to be the most promising for intravital video fluorescence monitoring of biotissues when performing this kind of laser delivery [12–14]. In addition to the analysis of coenzyme fluorescence signal inherent to biotissues, molecules and nanoparticles with fluorescent properties, photocytotoxic effect and selective accumulation by various cellular structures and tumour tissues in comparison with surrounding tissues are also of interest [15–18]. This approach significantly increases the diagnostic informative value of tumour tissue composition by recognising cancer cells and tumour associated macrophages/microglia (TAM) [19].

It is known that most tumour cells receive energy differently than healthy cells primarily because of differences in the glycolysis process. Tumour cells obtain energy through rapid anaerobic glycolysis with lactic acid formation, whereas in normal cells slow glycolysis occurs in the presence of oxygen through slow enzymatic reactions with the formation of two ATP molecules. Therefore, studies have been carried out to detect differences between tumour cells and immunocompetent cells, in particular tumour-associated macrophages (TAM) by the fluorescent signal of the coenzymes HADH and FAD (to which macrophages are enriched) and the difference in accumulation. FAD, NADH and NADH2 are important elements in cellular metabolism as well as endogenous fluorophores through which cell differentiation can be produced. The fluorescence of these coenzymes depends on their form and state. In addition, time-resolved spectroscopic analysis was also performed using the photosensitizer 5-ALA induced PpIX, which is widely used in clinical practice for effective fluorescence diagnosis (FD) and photodynamic therapy (PDT) [8–10]. Monitoring of fluorescence lifetime of PS before and after PDT (but with repeated administration of 5-ALA) was performed using a measuring complex based on a streamer camera with picosecond time resolution coupled to a fibre optic spectrometer. As a result, such a multifaceted approach made it possible to analyse the composition of tumour tissue, making assumptions based on the construction of tissue metabolic relationships and the resulting fluorescence lifetime data.

2. Materials and Methods

The monitoring of cell growth processes consists in the detection by fluorescence spectroscopy of areas with increased fluorescence intensity caused either by an increased concentration of accumulating photosensitizer molecules in the case of glioma or by a high concentration of nerve cells labelled with special fluorescent proteins. The study was performed on experimental animals (sexually mature female Wistar rats weighing 200–220 g) with an induced brain tumour. Animal care protocols were used in accordance with the guidelines of European Convention for the Protection of Vertebrate Animals used for Experimental and Other Scientific Purposes (Strasbourg, 18.III.1986).

In order to provide access to the tumour bed, an intracranial neurosystem with an internal fibre optic structure was preliminarily implanted. The fibre optic neurosystem thereby made it possible to perform in vivo measurements. Both autofluorescence signal of endogenous tissue fluorophores and fluorescence of exogenous fluorophores using Alasens®, synthesized by NIOPIK was recorded using the installed fibre optic neurosystem on the model of experimental animals with induced C6 glioma. Sterile aqueous PS solution for application, concentration c = 100 mg/kg, was prepared one hour before use by dissolving the required amount of Alasens® powder in 5% sterile sodium bicarbonate solution.

To study PS photoluminescence kinetics, a measurement setup based on a picosecond time-resolved (15 ps) Hamamatsu C10627-13 streamer coupled to a fibre optic spectrometer was previously developed. A Hamamatsu semiconductor laser with a pulse duration of 67 ps and a wavelength of 637 nm was used for excitation. During measurements we used a time-correlated single photon counting method. Photoluminescence excited in a sample

by a laser source is collected in an optical fibre and is then fed into a monochromator to obtain information about the lifetime of the fluorescence and the distribution of the number of photons recorded by the streamer between lifetime components.

In this work, the method of recording the fluorescence lifetime of NADH, FAD and PS used a FLIM attachment of laser scanning microscope, which allows evaluating lifetime distribution in each point of the sample under study. The actual localisation (accumulation area) and fluorescence spectrum of the PS or endogenous fluorophore is assessed by analysing the images taken by fluorescence microscopy. Fluorescence kinetic characteristics were studied using a laser scanning microscope LSM-710-NLO (Carl Zeiss, Jena, Germany). Excitation was performed with a femtosecond pulsed laser Chameleon Ultra II (80 MHz, pulse duration 140 fs, wavelength range 690–1060 nm, Coherent Inc., Santa Clara, CA, USA), wavelength 980 nm. Images were acquired with the following scanning modes: 20× objective, scan area size 400 × 400 μm, resolution 1024 × 1024 pixels, scan speed 1.27–3.15 μs/pixel. Total image acquisition time is 18.7 s. The average power density measured with a Coherent power meter (USA) at the sample location level was 5.42 mW, with a power density of 7 kW/cm^2 per scanning spot, 10 μm in size.

3. Results

3.1. Fluorescence Lifetime of Exogenous Fluorophores

Time-resolved spectroscopic analysis of the fluorescence lifetime was performed on female rats with glioma C6-induced brain tumour under in vivo conditions (Figure 1). 5-ALA induced Pp IX (NIOPIK), which is widely used in clinical practice for effective fluorescence diagnostics and PDT, was used as PS. 5-ALA was injected into experimental animals into tail vein at the dose of 10 mg/kg under general anaesthesia. The level of Pp IX accumulation in norm and tumour in vivo was monitored using LESA-01-Biospect fibre spectrometer (Figure 2a). As a result, photodynamic treatment with laser radiation (λ = 650 nm, dose 200 J/cm^2) was performed at the time of maximum accumulation (t = 3 h). Measurements were made in vivo by using a fibre optic neural system (Figure 1). Monitoring of fluorescence lifetime of PS before and after PDT (but with re-injection of 5-ALA) was carried out using a measuring complex based on a streamer camera with picosecond time resolution, coupled with a fibre-optic spectrometer. The time-correlated photon counting method was used in the measurement process.

(**a**) (**b**)

Figure 1. Image of the intracranial location of the fibre optic neural system after implantation: (**a**) schematic representation, (**b**) in vivo image on an experimental animal.

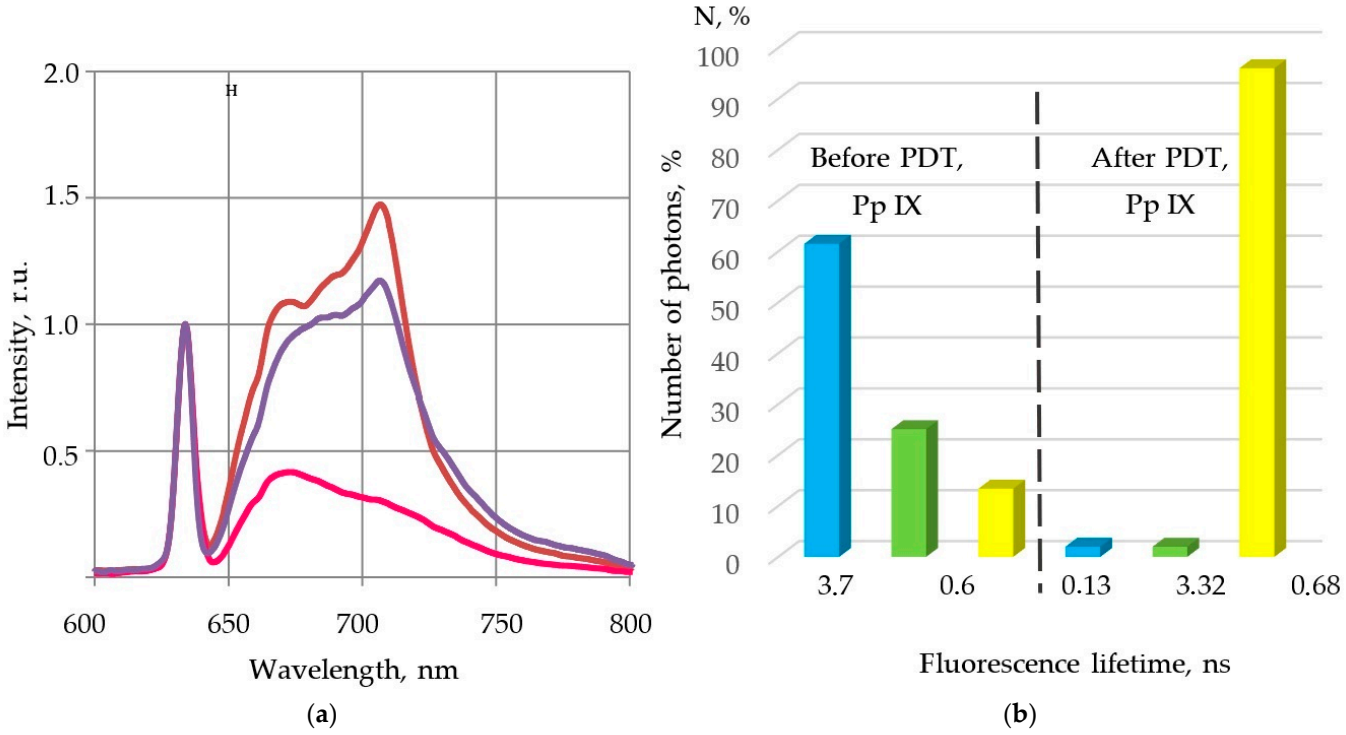

Figure 2. (**a**) PpIX fluorescence spectra characterising the accumulation of PS in a rat brain tumour (glioma C6)-before PDT, -after PDT, -after PDT while reintroducing PS. (**b**) Results of time-resolved spectroscopic analysis of PpIX fluorescence lifetime in a rat brain tumour, presented as a histogram of contribution from different components of fluorescence lifetime.

As a result, at the time of maximum accumulation (t = 3 h), photodynamic treatment with laser radiation (λ = 650 nm, dose 200 J/cm^2) was performed. The fluorescence lifetime of PS before and after PDT (but with re-injection of 5-ALA) was monitored using a measuring complex based on a streamer camera with picosecond time resolution, coupled with a fibre-optic spectrometer. The time-correlated photon counting method was used in the measurement process. Thus, results were obtained on the variation of the luminescence kinetics of PpIX under in vivo conditions in experimental animals with glioma C6 induced brain tumour. The presence of three different components characteristic of the fluorescence lifetime of PrIX was found, but the contribution (number of fluorescence photons) of each component was strongly dependent on the biological microenvironment and on the phenotype of the cells with which the fluorophore interacts. In addition, it was found that PDT and, as a consequence, changes in the metabolic processes within the cells resulted in changes in the contribution to the fluorescence kinetics of various temporal components, while the fluorescence lifetime itself did not change (Figure 2b). Based on the results obtained, the conclusion was made that there are constituents in the tumour that also actively accumulate PS, but interact with it in a different way. The role of such agents is primarily claimed by immunocompetent cells, namely macrophages due to their increased ability to accumulate PS.

This assumption was tested by analysing tumour cryosections before and after PDT [12,13] using confocal and time-resolved fluorescence microscopy (Figures 3a and 4a). As a result, fluorescence centres with lifetimes consistent with those previously obtained under in vivo conditions were detected before and after PDT (Figures 3b and 4b). The localization and morphology of the cells indicated their immune nature. Their close proximity to the tumour gave grounds to consider them as tumour-associated macrophages. Thus, the assessment of tissue cell composition in a non-invasive monitoring mode will enable selective deactivation of pathological cells (including immune cells), which will significantly increase the effectiveness of antitumour therapy. A special role in such studies can be played by the developed neuroport. A comprehensive approach in the assessment of the tumour bed

using a multifunctional neurosystem will allow the analysis of the cellular composition of tumour tissue at a significant depth in continuous monitoring mode, which will make significant progress in the effectiveness of brain tumours therapy.

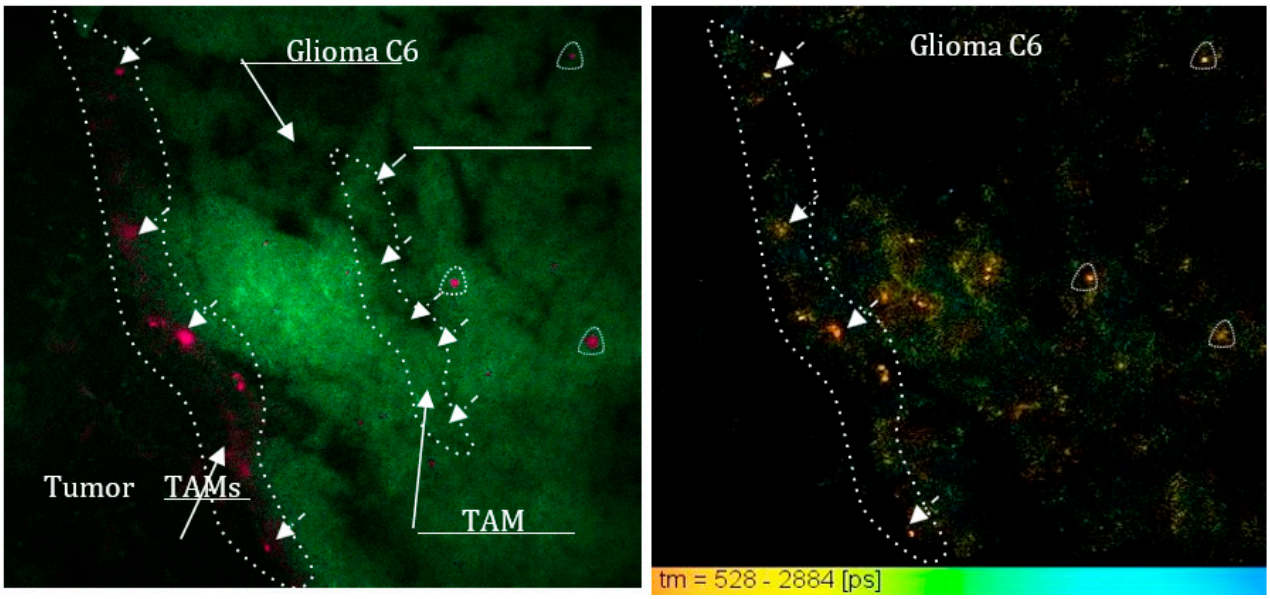

(**a**) (**b**)

Figure 3. (**a**) Fluorescence image of PpIX accumulation centres obtained from rat brain cryosections at the border of tumour and normal tissue by confocal microscopy (20× magnification): Red—Fluorescence in the area 660–720 nm indicating accumulation of PpIX; Green—Autofluorescence of tissue in the area 450–550 nm indicating live tissue retention. (**b**) Image of spatial distribution of fluorescence lifetime obtained from rat brain cryosections at the border of tumour and normal tissue by FLIM (20× magnification). The colour scale from orange to blue corresponds to an increase in the lifetime of the fluorescence from 528 ps to 2884 ps.

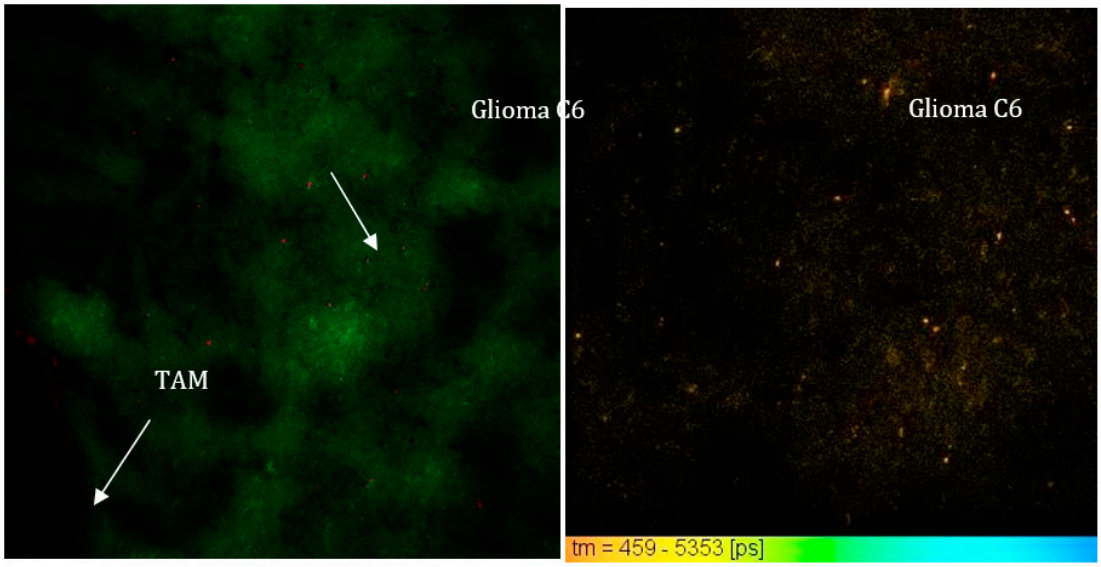

(**a**) (**b**)

Figure 4. (**a**) Fluorescence image of PpIX accumulation centres obtained from rat brain cryosections after PDT at the border of tumour and normal tissue by confocal microscopy (20× magnification): Red—Fluorescence in the area 660–720 nm indicating accumulation of PpIX; Green—Autofluorescence of tissue in the area 450–550 nm indicating live tissue retention. (**b**) Image of spatial distribution of fluorescence lifetime obtained from rat brain cryosections after PDT at the border of tumour and normal tissue by FLIM (20× magnification): The colour scale from orange to blue corresponds to an increase in the lifetime of the fluorescence from 450 ps to 5353 ps.

3.2. Fluorescence Lifetime of Endogenous Fluorophores

Tumour cells contain significant amounts of bound NADH, which has a long fluorescence lifetime, whereas immunocompetent cells (macrophages in particular) contain large amounts of FAD. Based on these properties, the imaging of macrophages in tumours in vivo was performed. The study of photoluminescence kinetics of NADH and FAD coenzymes using time-resolved fluorescence microscopy (FLIM) revealed that in certain large clusters of cells, apparently macrophages, the processes of oxidative phosphorylation (energy storage as ATP) prevail over the glycolysis process leading to a decrease in NADH levels and an increase in FADH2 levels. In tumour cells, which form the majority in the field of view in Figure 5, the reverse energy conversion processes occur and glycolysis prevails over oxidative phosphorylation reactions, resulting in an increase of NADH level and a decrease of FADN2 level, which is in general agreement with the theory of oxidative processes. Using FLIM imaging, coenzyme fluorescence lifetime was assessed: tumour cells containing significant amounts of bound NADN had a long fluorescence lifetime, while immunocompetent cells (in particular, macrophages) containing large amounts of FAD showed a short coenzyme fluorescence lifetime (Figure 6). Based on these properties, macrophages were visualised in the tumour.

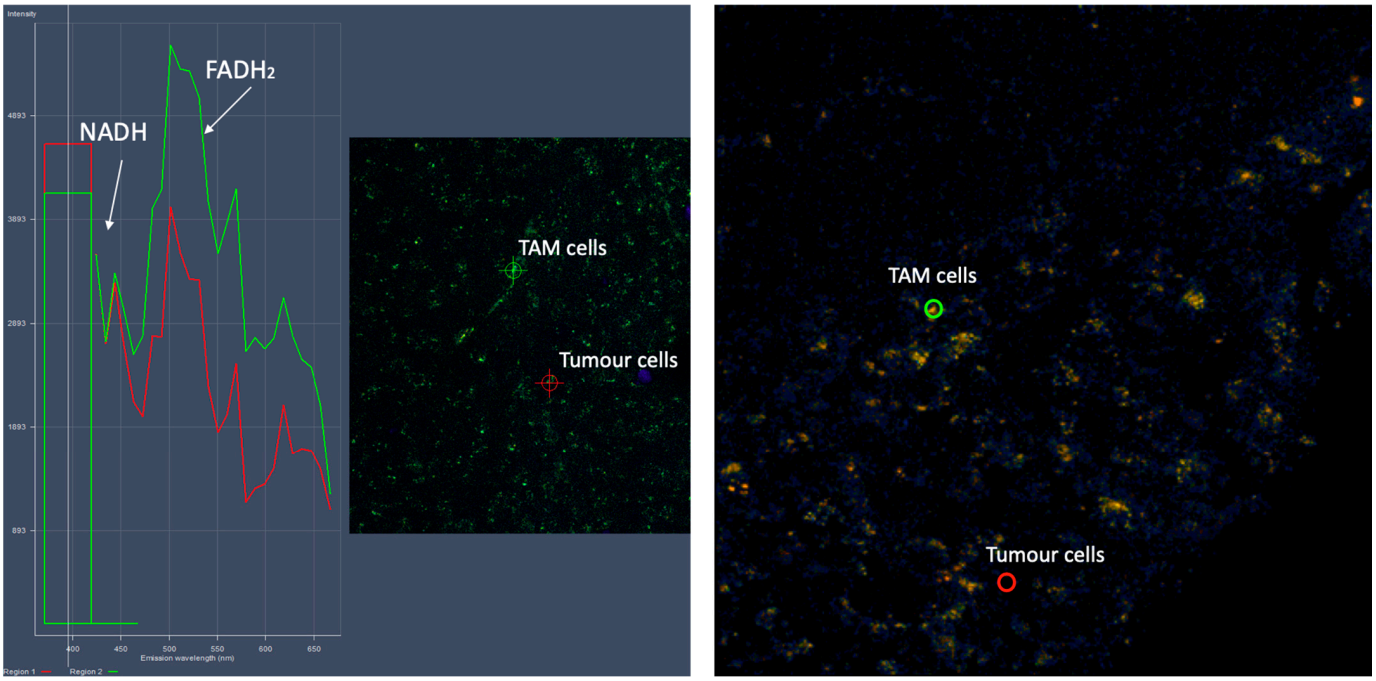

Figure 5. Fluorescence image characterised by spectral signal decomposition in individual fluorescent centres. Experimental samples in the form of cryosections were obtained from experimental animals: (**a**) coenzyme fluorescence spectra by the laser scanning microscope for different areas: cancer cell and TAM; (**b**) coenzyme fluorescence lifetime by FLIM for different areas: cancer cell and TAM.

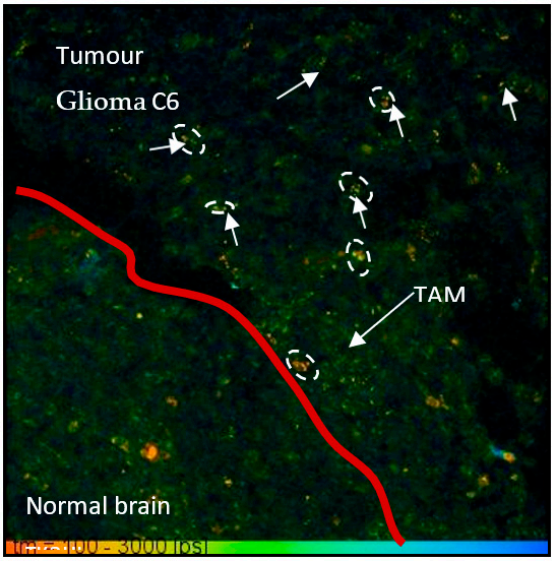

Figure 6. FLIM image characterising the fluorescence lifetime distribution of exogenous fluorophores in brain tissue at the border of C6 glioma tumour and normal tissue.

4. Discussion

The main aim of the research was to find spectral-luminescent features associated with metabolic changes that best reflect the state and composition of brain tumour tissue and serve as evidence-based prognostic factors. It can be seen that the initial results suggest that this tactic is promising for further development and use in the clinic.

These studies should provide a basis for finding a correspondence between the temporal fluorescence characteristics of PS absorbed by different cells within a tumour and the phenotype of these cells, in particular with the possibility to quantify the presence of tumour-associated microglia and macrophages in tumour tissue along with cancer cells. As a result, it will be established how the quantitative ratio of tumour-associated macrophages/microglia influences the pattern of tumour progression.

It is worth noting that recently there has been an increasing number of studies relating to the role of immunity in the development of tumours of different localization [20–23]. Particularly frequent studies have shown that the prognosis of gastrointestinal tumours depends on the composition of the tumour tissue [24–26]. In reality, immunity always interacts with a tumour in one way or another if it appears in the body [27–29]. In this regard, monitoring the course of the dialogue between cancer and immune cells is an important aspect both for practical purposes such as preventing metastasis, rehabilitating the overall normal immune response, as well as for the fundamental purposes of investigating the primary causes of tumour formation in any localization [30].

5. Conclusions

In the course of the study, it was shown that based on fluorescence lifetime measurements, both integral and local characteristics of fluorescence, it is possible to judge the metabolic activity of both individual cells and the composition of the whole tissue area. Based on this approach, spectral and temporal characteristics of fluorescence of fluorophores (both endogenous and PS) interacting with tumour-associated macrophages (TAM) have been obtained. In this context the methodology of in vivo tumour cell composition analysis seems to be promising, in particular the evaluation of such an important parameter as the quantitative content of TAM in tumour tissue, which in turn has an active influence on tumour progression. Photodynamic treatment has been shown to alter the metabolic activity of tissues, probably leading to the destruction of TAM that have accumulated PS, which is undoubtedly an important factor for new approaches to anti-tumour therapy.

Author Contributions: Data curation, Y.M. and V.L.; Funding acquisition, Y.M.; Investigation, Y.M., I.R. and A.S.; Methodology, Y.M. and D.F.; Project administration, V.L.; Supervision, V.L.; Writing—review & editing, Y.M. All authors have read and agreed to the published version of the manuscript.

Funding: This research was funded by RFBR according to the research project No. 21-52-15025.

Institutional Review Board Statement: Animal care protocols were used in accordance with the guidelines of European Convention for the Protection of Vertebrate Animals used for Experimental and Other Scientific Purposes (Strasbourg, 18.III.1986).

Informed Consent Statement: Not applicable.

Data Availability Statement: Not applicable.

Conflicts of Interest: The authors declare no conflict of interest.

References

1. Liu, H.; Hong, G.; Luo, Z.; Chen, J.; Chang, J.; Gong, M.; He, H.; Yang, J.; Yuan, X.; Li, L.; et al. Atomic-Precision Gold Clusters for NIR-II Imaging. *Adv. Mater.* **2019**, *31*, e1901015. [CrossRef] [PubMed]
2. Grosenick, D.; Wabnitz, H.; Macdonald, R. Diffuse near-infrared imaging of tissue with picosecond time resolution. *Biomed. Tech. Eng.* **2018**, *63*, 511–518. [CrossRef] [PubMed]
3. Lukina, M.; Yashin, K.; Kiseleva, E.E.; Alekseeva, A.; Dudenkova, V.; Zagaynova, E.V.; Bederina, E.; Medyanic, I.; Becker, W.; Mishra, D.; et al. Label-Free Macroscopic Fluorescence Lifetime Imaging of Brain Tumors. *Front. Oncol.* **2021**, *11*, 1781. [CrossRef] [PubMed]
4. Haidar, D.A.; Leh, B.; Zanello, M.; Siebert, R. Spectral and lifetime domain measurements of rat brain tumors. *Biomed. Opt. Express* **2015**, *6*, 1219–1233. [CrossRef]
5. Hatami, N.; Sun, Y.H.; Yee, M.; Phipps, J.E.; Elson, D.; Gorin, F.; Schrot, R.J.; Marcu, L. Fluorescence lifetime imaging microscopy for brain tumor image-guided surgery. *J. Biomed. Opt.* **2010**, *15*, 056022. [CrossRef]
6. Alfonso-Garcia, A.; Bec, J.; Weaver, S.S.; Hartl, B.; Unger, J.; Bobinski, M.; Lechpammer, M.; Girgis, F.; Boggan, J.; Marcu, L. Real-time augmented reality for delineation of surgical margins during neurosurgery using autofluorescence lifetime contrast. *J. Biophotonics* **2020**, *13*, e201900108. [CrossRef]
7. Schroeder, A.B.; Pointer, K.B.; Clark, P.A.; Datta, R.; Kuo, J.S.; Eliceiri, K.W. Metabolic mapping of glioblastoma stem cells reveals NADH fluxes associated with glioblastoma phenotype and survival. *J. Biomed. Opt.* **2020**, *25*, 036502. [CrossRef]
8. Erkkilä, M.T.; Reichert, D.; Hecker-Denschlag, N.; Wilzbach, M.; Hauger, C.; Leitgeb, R.A.; Gesperger, J.; Kiesel, B.; Roetzer, T.; Widhalm, G.; et al. Surgical microscope with integrated fluorescence lifetime imaging for 5-aminolevulinic acid fluorescence-guided neurosurgery. *J. Biomed. Opt.* **2020**, *25*, 071202. [CrossRef]
9. Erkkilä, M.T.; Bauer, B.; Hecker-Denschlag, N.; Medina, M.J.M.; Leitgeb, R.A.; Unterhuber, A.; Gesperger, J.; Roetzer, T.; Hauger, C.; Drexler, W.; et al. Widefield fluorescence lifetime imaging of protoporphyrin IX for fluorescence-guided neurosurgery: An ex vivo feasibility study. *J. Biophotonics* **2019**, *12*, e201800378. [CrossRef]
10. Erkkilä, M.T.; Reichert, D.; Gesperger, J.; Kiesel, B.; Roetzer, T.; Mercea, P.A.; Drexler, W.; Unterhuber, A.; Leitgeb, R.A.; Woehrer, A.; et al. Macroscopic fluorescence-lifetime imaging of NADH and protoporphyrin IX improves the detection and grading of 5-aminolevulinic acid-stained brain tumors. *Sci. Rep.* **2020**, *10*, 20492. [CrossRef]
11. Sharova, A.; Maklygina, I.S.; Ryabova, A.V.; Loschenov, V.; Romanishkin, I.; Yusubalieva, G.; Chekhonin, V. Optical fiber neurosystem for deep-lying brain tumors phototheranostics. *Opt. Instrum. Sci. Technol. Appl.* **2018**, *10695*, 106950O. [CrossRef]
12. Markosian, C.; Mazzola, C.A.; Tomycz, L.D. Sodium Fluorescein-Guided Gross Total Resection of Pediatric Exophytic Brainstem Glioma: 2-Dimensional Operative Video. *Oper. Neurosurg.* **2020**, *20*, E146–E147. [CrossRef]
13. Sun, Z.; Jing, L.; Fan, Y.; Zhang, H.; Chen, L.; Wang, G.; Sharma, H.S.; Wang, J. Fluorescein-guided surgery for spinal gliomas: Analysis of 220 consecutive cases. *New Concepts Psychostimulant Induc. Neurotox.* **2020**, *151*, 139–154. [CrossRef]
14. Valdes, P.A.; Millesi, M.; Widhalm, G.; Roberts, D.W. 5-aminolevulinic acid induced protoporphyrin IX (ALA-PpIX) fluorescence guidance in meningioma surgery. *J. Neuro-Oncol.* **2019**, *141*, 555–565. [CrossRef]
15. Li, X.; Fan, H.; Guo, T.; Bai, H.; Kwon, N.; Kim, K.H.; Yu, S.; Cho, Y.; Kim, H.; Nam, K.T.; et al. Sequential Protein-Responsive Nanophotosensitizer Complex for Enhancing Tumor-Specific Therapy. *ACS Nano* **2019**, *13*, 6702–6710. [CrossRef]
16. Jung, S.; Jung, S.; Kim, D.M.; Lim, S.-H.; Shim, Y.H.; Kwon, H.; Kim, D.H.; Lee, C.-M.; Kim, B.H.; Jeong, Y.-I. Hyaluronic Acid-Conjugated with Hyperbranched Chlorin e6 Using Disulfide Linkage and Its Nanophotosensitizer for Enhanced Photodynamic Therapy of Cancer Cells. *Materials* **2019**, *12*, 3080. [CrossRef] [PubMed]
17. Lee, S.J.; Jeong, Y.I. Hybrid nanoparticles based on chlorin e6-conjugated hyaluronic acid/poly(l-histidine) copolymer for theranostic application to tumors. *J. Mater. Chem. B* **2018**, *6*, 2851–2859. [CrossRef] [PubMed]
18. Kook, M.-S.; Lee, C.-M.; Jeong, Y.-I.; Kim, B.-H. Nanophotosensitizers for Folate Receptor-Targeted and Redox-Sensitive Delivery of Chlorin E6 against Cancer Cells. *Materials* **2020**, *13*, 2810. [CrossRef] [PubMed]

19. Sørensen, M.D.; Dahlrot, R.H.; Boldt, H.B.; Hansen, S.; Kristensen, B.W. Tumour-associated microglia/macrophages predict poor prognosis in high-grade gliomas and correlate with an aggressive tumour subtype. *Neuropathol. Appl. Neurobiol.* **2018**, *44*, 185–206. [CrossRef]
20. Pan, Y.; Yu, Y.; Wang, X.; Zhang, T. Tumor-Associated Macrophages in Tumor Immunity. *Front. Immunol.* **2020**, *11*, 583084. [CrossRef]
21. Maller, O.; Drain, A.P.; Barrett, A.S.; Borgquist, S.; Ruffell, B.; Zakharevich, I.; Pham, T.T.; Gruosso, T.; Kuasne, H.; Lakins, J.N.; et al. Tumour-associated macrophages drive stromal cell-dependent collagen crosslinking and stiffening to promote breast cancer aggression. *Nat. Mater.* **2021**, *20*, 548–559. [CrossRef]
22. Anderson, N.R.; Minutolo, N.G.; Gill, S.; Klichinsky, M. Macrophage-Based Approaches for Cancer Immunotherapy. *Cancer Res.* **2021**, *81*, 1201–1208. [CrossRef]
23. Cersosimo, F.; Lonardi, S.; Bernardini, G.; Telfer, B.; Mandelli, G.E.; Santucci, A.; Vermi, W.; Giurisato, E. Tumor-Associated Macrophages in Osteosarcoma: From Mechanisms to Therapy. *Int. J. Mol. Sci.* **2020**, *21*, 5207. [CrossRef]
24. Yahaya, M.A.F.; Lila, M.A.M.; Ismail, S.; Zainol, M.; Afizan, N. Tumour-Associated Macrophages (TAMs) in Colon Cancer and How to Reeducate Them. *J. Immunol. Res.* **2019**, *2019*, 2368249. [CrossRef]
25. Lin, C.; He, H.; Liu, H.; Li, R.; Chen, Y.; Qi, Y.; Jiang, Q.; Chen, L.; Zhang, P.; Zhang, H.; et al. Tumour-associated macrophages-derived CXCL8 determines immune evasion through autonomous PD-L1 expression in gastric cancer. *Gut* **2019**, *68*, 1764–1773. [CrossRef]
26. Wei, C.; Yang, C.; Wang, S.; Shi, D.; Zhang, C.; Lin, X.; Liu, Q.; Dou, R.; Xiong, B. Crosstalk between cancer cells and tumor associated macrophages is required for mesenchymal circulating tumor cell-mediated colorectal cancer metastasis. *Mol. Cancer* **2019**, *18*, 64. [CrossRef]
27. Krump, N.A.; You, J. Molecular mechanisms of viral oncogenesis in humans. *Nat. Rev. Genet.* **2018**, *16*, 684–698. [CrossRef] [PubMed]
28. Greten, F.R.; Grivennikov, S.I. Inflammation and Cancer: Triggers, Mechanisms, and Consequences. *Immunity* **2019**, *51*, 27–41. [CrossRef] [PubMed]
29. Hojman, P.; Gehl, J.; Christensen, J.F.; Pedersen, B.K. Molecular Mechanisms Linking Exercise to Cancer Prevention and Treatment. *Cell Metab.* **2018**, *27*, 10–21. [CrossRef] [PubMed]
30. Petty, A.J.; Yang, Y. Tumor-associated macrophages: Implications in cancer immunotherapy. *Immunotherapy* **2017**, *9*, 289–302. [CrossRef] [PubMed]